*Optica Applicata, Vol. XXXIV, No. 3, 2004*

# Electrical substitution cryogenic radiometer based spectral responsivity scale between 250–2500 nm wavelengths

ÖZCAN BAZKIR, FARHAD SAMEDOV

TUBITAK-Ulusal Metroloji Enstitüsü (UME), P.O. Box. 54 41470 Kocaeli/Turkey
e-mail: ozcanb@ume.tubitak.gov.tr

This paper presents the spectral responsivity scale between 250–2500 nm developed by the National Metrology Institute of Turkey (UME). For that purpose silicon photodiode based trap detector and electrically calibrated pyroelectric radiometer (ECPR) that were calibrated against primary level absolute electrical substitution cryogenic radiometer (ESCR) were used as transfer standards. Using highly collimated and stabilized ($10^{-5}$) lasers, absolute optical powers and absolute responsivity of trap detector were measured with an uncertainty of the order of $10^{-4}$. In visible (VIS) region responsivity scale was set by means of the models for the reflectance and internal quantum efficiency. In the ultraviolet (UV) and near-infrared (NIR) regions spectrally flat (0.1%) ECPR was used.

Keywords: electrical-substitution cryogenic radiometer, electrically calibrated pyroelectric radiometer, trap detector, radiant source, optical power, responsivity.

## 1. Introduction

In metrology the candela, the SI unit of luminous intensity, is determined in terms of the absolute responsivity of detector from the absolute measurement of optical power using ESCR's working at liquid helium temperatures (4.2 K) [1]–[5]. At this temperature, the uncertainty in the optical power measurements is of the order of 0.005% [1], [6]. Responsivity standards have been changed significantly in the past two decades from single element detectors to reflection or transition type trap detectors. Compared to other optical radiation detectors, trap detectors constructed from silicon photodiodes have better optical properties [7], [8]. Having good stability, uniformity, linearity and spectral response to intensity from $10^{-13}$ W/cm$^2$ to 10 mW/cm$^2$, these detectors have been used in many applications starting from the deep UV through the VIS to the NIR.

In UV and NIR regions there are some problems with decreasing internal quantum efficiency of silicon photodiodes, which brings about high errors in the interpolation

of spectral responsivity using the physical models developed [9]–[11]. In order to measure optical radiation in UV and IR regions ECPR have been used as a transfer standard. It can measure the total power and irradiance of cw sources. The most common application for the ECPR is to transfer an absolute radiometric calibration to another detector or light source with a high degree of accuracy. This is accomplished by measuring either the total power (watts) of collimated sources that under fill the detector aperture or the irradiance ($W/cm^2$) of extended sources that overfill the detector aperture. The exceptionally flat spectral response ensures that broadband sources are measured with the same accuracy as monochromatic light, allowing the ECPR to calibrate VIS and IR detectors, standard lamps, blackbody emitters, laser power meters, UV exposure meters, *etc.* [12].

In this paper, we present both optical power and responsivity measurements necessary for the realization of spectral responsivity scale. Our absolute responsivity scale is based on home-made reflection type reference trap detectors calibrated against ESCR. The scale was obtained using suitable mathematical models for the calculated internal quantum efficiency from measured absolute responsivity values and reflectance measurements at the laser wavelengths. The relative responsivity scale is based on ECPR absolutely calibrated against ESCR at laser wavelengths and the spectral responsivity scale of ECPR was expanded by measuring the change in the pyroelectric detector's reflectance.

## 2. Absolute optical power measurements

The optical power measurement system consists of two parts; a laser power stabilizer (LPS) system and an electrical substitution cryogenic radiometer (ESCR), which is designed such that it can be used with a beam of collimated and vertically polarized light with powers ranging from a few μW to 1 mW. As radiant sources we used $Ar^+$ (488 nm and at 514.5 nm), Nd:YAG (with second harmonic 532 nm), and He-Ne (632.8 nm) lasers in the measurement. LPS shown in the Fig. 1 was used for compensation of fluctuations in the optical power and generation of a geometrically well-defined Gaussian laser beam. The LPS consists of an electro-optic modulator (EOM), temperature controlled monitor photodiode and control electronics. Vertically polarized laser light incident on the EOM first passes through a liquid crystal, which alters the beam transmittance, then passes through a beam splitter, which transmits 98% of the incident light. The optical beam after passing through the EOM is partially reflected from the wedged fused-silica beam splitter. A precision monitor photodiode receives the reflected beam from the wedged window and sends it back to the EOM. This feedback loop controls the optical beam to get a constant signal power output. Using this technique the output stability level reached was of the order of $6\times10^{-5}$. The spatial profiles of the beams were purified with spatial filter. The diameters of the beams after spatial filter are close to 3 mm ($1/e^2$ points).

The entrance window of the ESCR is a fussed silica glass aligned to Brewster angle. Before measurements the window was released and cleaned using suitable solutions

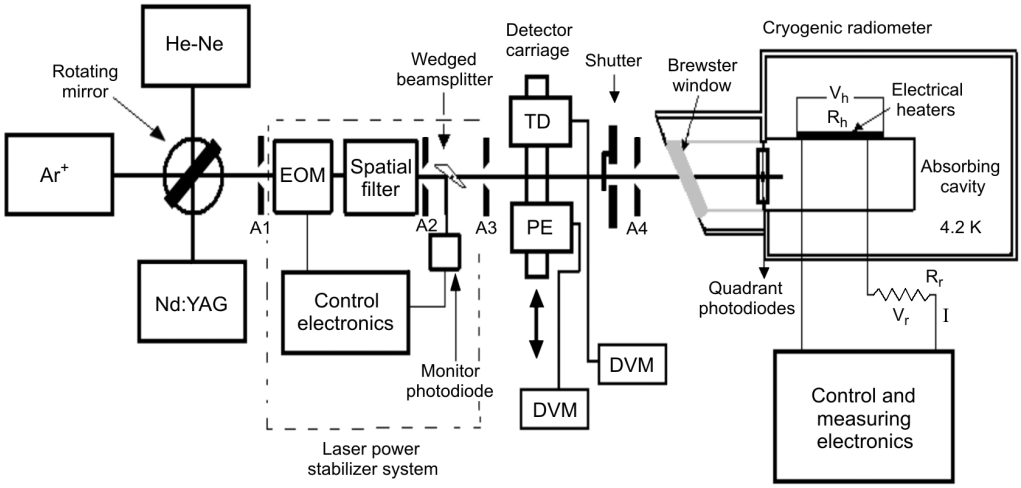


Fig. 1. Experimental set-up for optical power measurements. The symbols TD and PE denote trap detector and pyroelectric, respectively; A1, A2, A3 and A4 are apertures; $R_h$ and $R_r$ ($V_h$ and $V_r$) are the heater and reference resistances (voltages), respectively; $I$ is the current; DVM is digital multimeter; EOM is electro -optics modulator.

like ethanol, and lens paper with drop and drag method [13] and its transmittance measured was better than 99.9%. Laser beams enter the cavity by passing through quadrant photodiodes operating at photovoltaic mode. The scattered part of signals that have not entered to the absorbing cavity are incident on the quadrant photodiodes. These signals were calculated and applied as a correction factor to the measured power from cavity. The temperature of absorbing cavity was reduced to 4.2 K. The low operating temperature causes a dramatic increase in the sensitivity of the thermal sensor, reduces the cavity's thermal capacity and minimizes the effect of background radiation. The temperature of the cavity was measured using the temperature sensors on the cavity.

The operating principle of ESCR is that during the alternate radiant and electrical heating cycles electrical power is adjusted by the current passed through series resistance so that the temperature recorded by the temperature sensor is the same for electrical and optical heatings. Then, the radiant power is equated to the measured quantity of electrical power. The measured electrical power is calculated from the following equation [14]:

$$P_E = V_h \times I = V_h \frac{V_s}{R_s} \tag{1}$$

where $R_h$ and $R_r$ ($V_h$ and $V_r$) are heater and reference resistances (voltages), respectively; $I$ is the current.

Since the optical radiation $P_{\text{opt}}$ can be reduced by scattering $S(\lambda)$, by the window transmittance $\tau(\lambda)$ ,by the optical electrical non equivalence $N$ and imperfect cavity

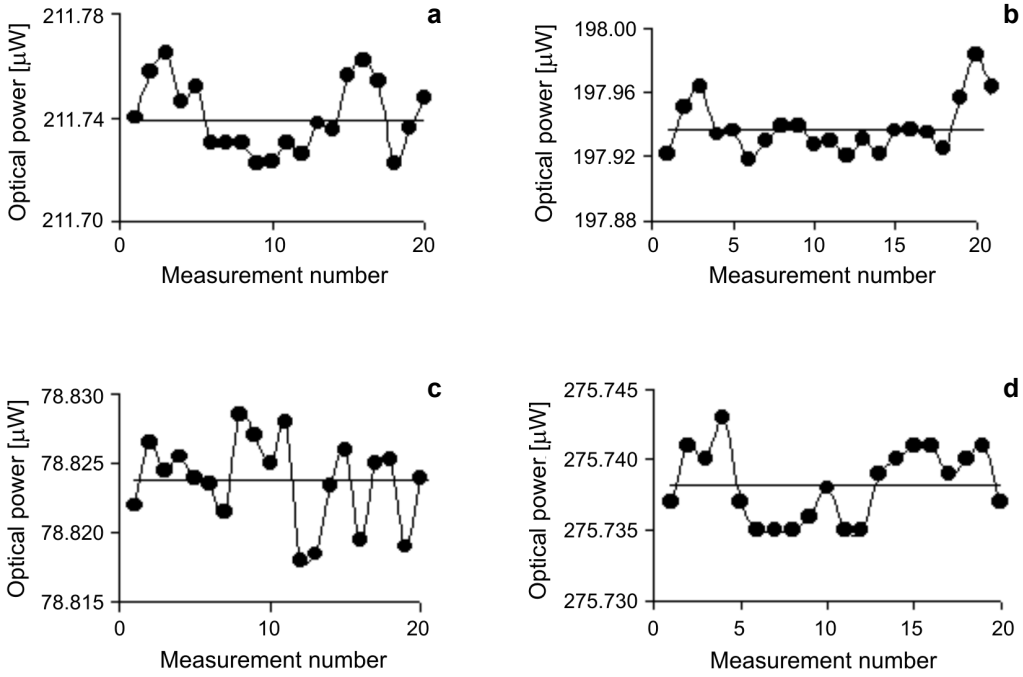


Fig. 2. Illustration of the optical power measurement results: **a** – $Ar^+$ (488 nm), **b** – $Ar^+$ (514.5 nm), **c** – Nd:YAG (532 nm), **d** – He-Ne (632.8 nm).

absorbance $\alpha(\lambda)$, the measured optical power should be corrected for these parameters [15]. The resultant optical power can be obtained as follows:

$$P_{\text{corr.opt}}(\lambda) = \frac{1}{\tau(\lambda)}\left[\frac{NP_{\text{opt}}}{\alpha(\lambda)} + S(\lambda)\right]. \tag{2}$$

The optical power measurements of the laser beams used are shown in Fig. 2. In order to minimize errors from power fluctuations, measurement cycles were repeated twenty times.

## 3. Responsivity measurements

### 3.1. Absolute responsivity measurements

Because silicon photodiode based reflection type trap detectors have good spatial uniformity, good temporal stability, low nonlinearity, low noise equivalent power, low reflectance, polarization independency, high quantum efficiency and predicted spectral responsivity in the visible region they have been used to link the high accuracy measurements obtained from the ESCR system to the other optical power measurement systems in the visible region [16], [17]. It is known that silicon photodiodes are used

for photon detection between 250–1100 nm wavelength and internal quantum efficiency is relatively flat (nearly equal to 100%) between 350–850 nm wavelengths, which allows the spectral responsivity to be interpolated throughout this range [18]. In UV and NIR regions, there are some problems with decreasing internal quantum efficiency of silicon photodiodes, which brings about high errors in the interpolation of spectral responsivity using the physical models developed [9]–[11]. In order to measure optical radiation in UV and IR regions pyroelectric radiometers (detectors) have been used as a transfer standard for the ultraviolet, visible and mid-infrared ranges [19].

In order to measure the absolute responsivities, both detectors were placed on the computer-controlled stage (Fig. 1) and after the measurement of optical power with ESCR the detector moved in the beam position and photocurrents were measured. Dividing photocurrent to the optical power absolute responsivities of detectors at 488, 514.5, 532, and 632.8 nm laser wavelengths were obtained.

### 3.2. Extrapolation and interpolation of absolute responsivities of trap detector

In order to realize spectral responsivity scale, trap detectors consisting of three Hamamatsu S1337-11 windowless photodiodes were constructed as shown in Fig. 3. The number of photodiodes and their geometrical arrangements are determined so as to remove the polarisation sensitivity of trap detectors to incident light and reduce the high reflection losses of silicon photodiodes, which is about 30% in the visible region [20], and thereby increase external quantum efficiency. In this kind of trap detectors incoming beam undergoes five reflections where most of the radiation is being absorbed by photodiodes and the remaining beam returns back along the incoming beam. It is for these reasons that the response of the detector to incident light can be determined more effectively.

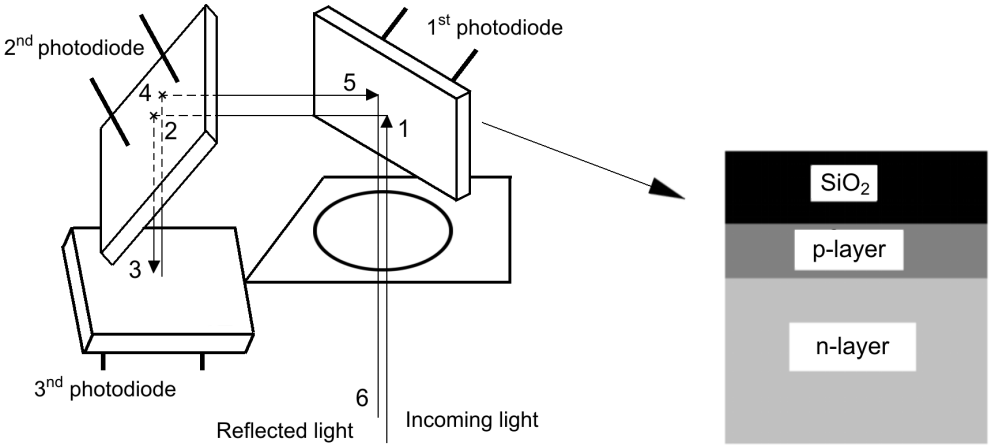


Fig. 3. Internal structure of trap detector and photodiode.

The spectral responsivity $R(\lambda)$ of trap detector in terms of reflectance and internal losses is given by [21]

$$R = \left[1 - \rho(\lambda)\right]\left[1 - \delta(\lambda)\right] \frac{e\lambda}{hc} \tag{3}$$

where $e$ is the elementary charge, $\lambda$ – the wavelength in vacuum, $h$ – the Planck constant, $c$ – the speed of light in vacuum, $\rho(\lambda)$ – the spectral reflectance, $\delta(\lambda)$ – the internal quantum deficiency of trap detector, and $1 - \delta(\lambda)$ is the internal quantum efficiency.

Spectral responsivity of a trap detector as given in Eq. (3) is defined with the reflectance and the internal quantum efficiency. These parameters have to be modelled so as to interpolate and extrapolate the absolute responsivity data.

#### 3.2.1. Measurement and modelling of reflectance losses

The reflectance of trap detectors was measured by means of $Ar^+$ (at 488 nm and 514.5 nm wavelengths), Nd:YAG (at 532 nm wavelength) and He-Ne (at 632.8 nm wavelength) lasers using the set-up shown in Fig. 4**a**. A stabilized laser beam was aligned towards a point close to the rim of a mirror. The beam reflected from the mirror fell on the trap detector and direct signal was measured with this detector. Than the beam reflected from the trap detector was measured using another trap detector. The measurements were repeated by interchanging the detectors. The repeatability in these

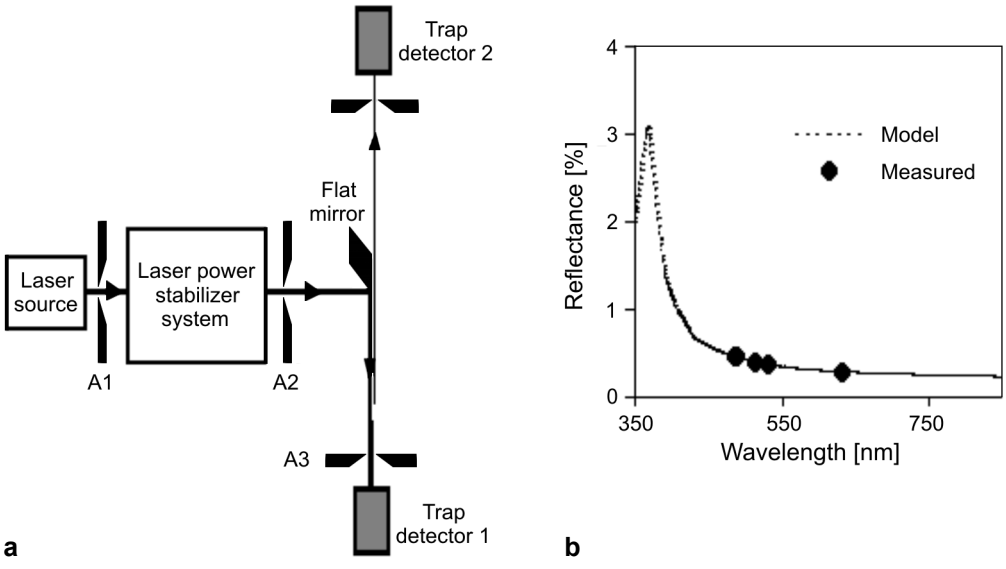


Fig. 4. Laser based spectral reflectance measurement set-up; A1, A2, A3 and A4 are the apertures (**a**). Illustration of reflectance of silicon photodiode based trap detector. Solid line indicates the theoretical model fitted to the measured values and black points indicate the measured data at laser wavelengths (**b**).

measurements was of the order of $10^{-4}$. The measurement results are displayed in Fig. 4**b**. In order to use these measured reflectance values in Eq. (3) for the realization of spectral responsivity scale these reflectance values have to be modelled. This is achieved as follows. In a trap detector, incoming beam undergoes five reflections due to the geometry of device (Fig. 3). The angle of incidence of these reflections is twice 45° for the perpendicular (*s*) plane of polarization, once normal incidence, and twice 45° for the parallel (*p*) plane of polarization. Thus, the reflectance of a trap detector is written as

$$\rho_{\mathrm{ref}} = \rho(0°)\rho_s^2(45°)\rho_p^2(45°). \tag{4}$$

To calculate these $\rho(0°)$, $\rho_s(45°)$ and $\rho_p(45°)$ reflections Fresnell's reflection, transmission equations and known refractive indices of Si and $SiO_2$ were used [20].

The calculated reflectance data were fitted to the measured data by adjusting the oxide thickness parameter. The difference between measured and calculated data after the best fit was at $10^{-4}$ level. The oxide thickness after the fitting was obtained as 28.08 nm. As shown in Fig. 4**b**, the reflectance of trap detector above about 400 nm is below 0.5%, which means that in this region the responsivity is insensitive to the reflectance changes, but increases at short wavelengths.

#### 3.2.2. Calculation and modelling of internal quantum efficiency

Quantum efficiency is defined as the ratio of countable events produced to the number of photons incident on the detector. The most important advantage of silicon based trap detectors is that internal quantum efficiency (IQE) is close to unity in the visible range [22]–[24]. This means that the spectral responsivity of trap detectors would not be changed in time and it would be linear over many orders of irradiance. Any deflection from unity is called internal quantum deficiency, which is assumed to be due to the trap charges at the $SiO_2$/Si interface [8]. This charge attracts the electrons (the minority carrier in this region) and reduces the number reaching the depletion region. To calculate the quantum efficiency of the photodiode it is necessary to quantify this loss mechanism. The IQE is related to the responsivity by the equation:

$$\mathrm{IQE} = 1 - \delta(\lambda) = \frac{Rhc}{\left[1 - \rho(\lambda)\right]e\lambda}. \tag{5}$$

In Eq. (5) the absolute responsivity values were obtained by measuring the trap detector response in terms of either current or voltage against the absolute optical power from ESCR at power stabilized $Ar^+$ (488 nm, 514.5 nm), Nd:YAG (at 532 nm) and He-Ne (632.8 nm) lasers. Using these responsivity values and reflectance $\rho$ values measured as described in Sections 3.1 and 3.2.1 the IQE values were calculated. In order to expand the IQE between 350 to 850 nm (Fig. 5**a**), the model described by Geist [22], [25], [26] was used, which is given as:

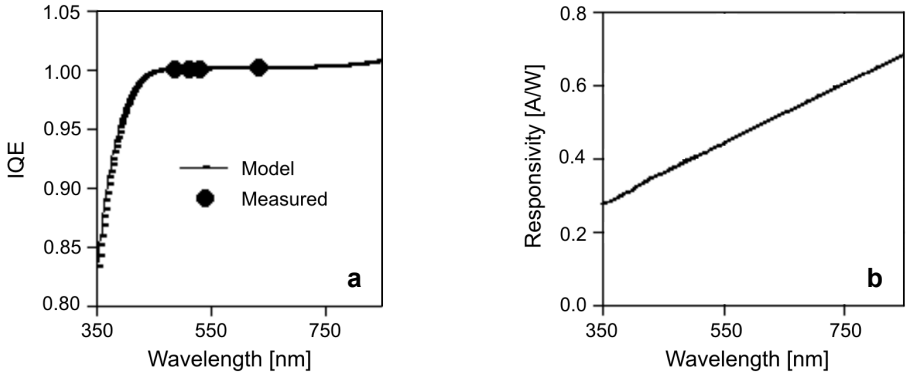


Fig. 5. Measured and modelled IQE of trap detector (**a**). Responsivity of trap detector between 350–850 nm wavelengths obtained from the combination of measured and modelled values (**b**).

$$\mathrm{IQE} = 1 - \delta = K\left[A_1 \exp\left(-\frac{\lambda}{\lambda_1}\right) + A_2 \exp\left(-\frac{\lambda^2}{\lambda_2^2}\right)\right]. \tag{6}$$

This equation is fitted to the IQE values obtained from Eq. (5) by adjusting the parameters $K$, $A_1$, $A_2$, $\lambda_1$ and $\lambda_2$.

Having seen that both the internal quantum efficiency and the reflectance of trap detector obtained effectively by the combination of measurements and the models developed, the spectral responsivity scale can be realized using Eqs. (3), (4) and (6). Comparing the calculated and measured values, a good agreement between them was observed. Hence we decided to use this model for the realization of spectral responsivity from 350 to 850 nm as shown in Fig. 5**b**.

### 3.3. Spectral responsivity measurement of ECPR

Pyroelectric materials are inherently spectrally flat over a broad wavelength range. Therefore the spectral responsivity of a pyroelectric detector is dependent on reflectance of the face electrodes and other materials placed on the detector surface to efficiently convert optical energy into thermal energy. The absorbance of the gold black coating determines the relative spectral responsivity, provided the transmition through the detector is negligible and the reflectance is low. Then the relative spectral response of the detector can be determined from a spectral reflectance measurement, assuming that the gold black transmittance is negligible and the relative detector response is proportional to 1 minus the measured reflectance and transmittance. Using the law of conservation of energy the absorption $\alpha_p(\lambda)$ is given as [27]

$$\alpha_p(\lambda) = 1 - \rho_p(\lambda) - \tau_p(\lambda) \tag{7}$$

where $\rho_p(\lambda)$ is the reflectance and the transmittance $\tau_p(\lambda)$ is assumed to be equal to zero. The predicted spectral responsivity $R_p(\lambda)$ of the pyroelectric detector is [27]

$$R_p(\lambda) = \left[1 - \rho_p(\lambda)\right] \mathrm{CF}_p \quad \left[\frac{\mathrm{A}}{\mathrm{W}}\right] \tag{8}$$

where $\mathrm{CF}_p$ is the pyroelectric calibration factor (absolute responsivity), which scales the output signal to the optical power received by the pyroelectric detector, being determined by calibrating ECPR against ESCR. The values of $\mathrm{CF}_p$ at laser wavelengths shown in Fig. 7**a** are about 1.005.

#### 3.3.1. Reflectance measurements of ECPR

The spectral reflectance of ECPR between the wavelengths of 250 and 2500 nm was measured using a measurement facility consisting of a double monochromator, a collimator, integrating sphere, a lock in amplifier, ECPR head and detector system as shown in Fig. 6. As a light source a flat tungsten filament quartz halogen lamp was used and it was operated at constant current mode, which kept the output from the lamp stable to within a few tenths of percent over a measurement period.

Light was focused onto the entrance slit of double-monochromator by using a spherical concave and cylindrical concave mirrors. The purpose of the cylindrical mirror is to correct astigmatism of the optical system. The light emitted by the source and reflected by the condensing mirrors passes through the order-sorting filter wheel after reaching the entrance slit. The order sorting filters are interchanged at nominal wavelengths to stop the radiation from higher-order diffraction of spectrum that would overlap with the working range. The flat mirror diverts the light from the slit to the first collimating mirror, which in turn illuminates the diffraction grating by a parallel white light beam.

The gratings disperse the light and a narrow-band (near-monochromatic) beam is focused to the entrance slit of the second half by the second collimating mirror and via

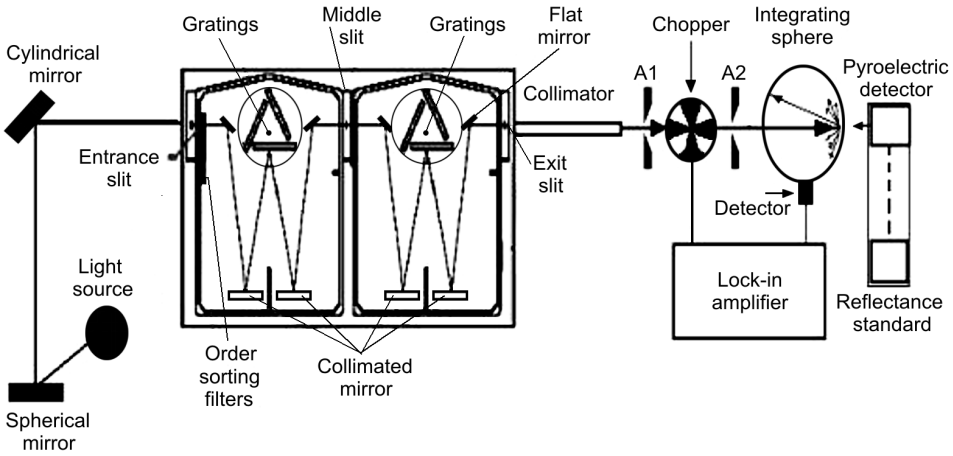


Fig. 6. Reflectance measurement set-up for the determination of the reflectance of pyroelectric detector (A1 and A2 are the apertures).

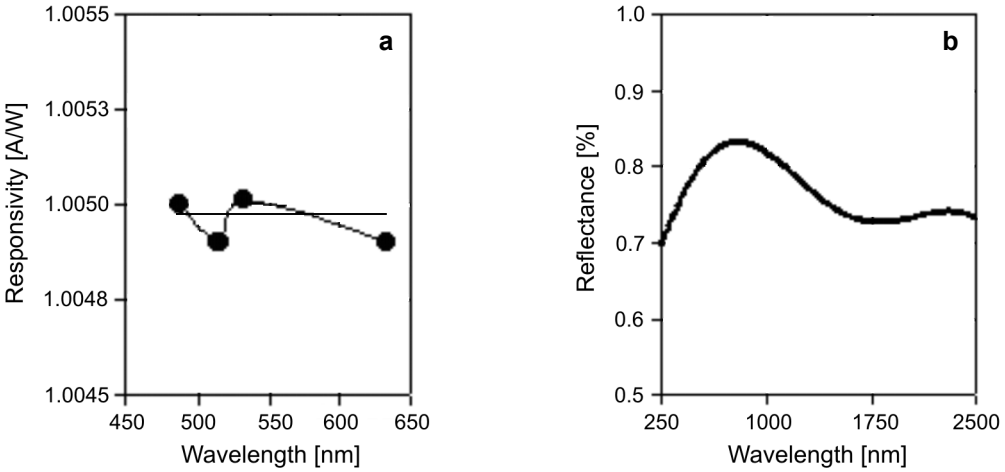


Fig. 7. Spectral reflectance of gold-black coated pyroelectric detector *vs.* wavelength (**a**); responsivity of pyroelectric detector (**b**).

a rotary flat mirror. In the second monochromator, the beam is again dispersed and directed to the exit slit by collimating and flat mirrors. The light beam emerging from the slit is collimated using collimators. In order to prevent scattered light small limiting circular apertures were used. The collimated beam was incident on the pyroelectric detector and reflection standard white barium sulphate ($BaSO_4$) plate, respectively. Reflected beams from the pyroelectric detector and reference standard were collected in the integrating sphere separately and these signals were recorded using silicon photodiode trap detector, InGaAs and HgCdTe detectors depending on wavelength range together with lock-in amplifier and chopper system. The spectral reflectance of ECPR at each wavelength was calculated from the averages of 50 measured reflectance values (Fig. 7**b**). The reflectance $\rho$ at wavelength $\lambda$ was calculated using the following equation:

$$\rho = \frac{A_{\mathrm{pd}}(\lambda) - A_{\mathrm{b}}(\lambda)}{A_{\mathrm{sd}}(\lambda) - A_{\mathrm{b}}(\lambda)} \tag{9}$$

where $A_{\mathrm{sd}}(\lambda)$ is the average reflected signal of the white standard, $A_{\mathrm{pd}}(\lambda)$ – the average reflected signal of the pyroelectric detector, and $A_{\mathrm{b}}(\lambda)$ is the average signal of the background.

Assuming the gold black transmittance of pyroelectric detector is negligible we have determined the relative spectral response (Fig. 8**a**) of the detector from a spectral reflectance measurement using Eq. (8). In the 250–2500 nm region the reflectance measurements indicated that the gold black coating is spectrally flat within 0.1%.

Employing the pyroelectric radiometer allows us to derive responsivity scale between 250 and 400 nm using silicon photodiode detector and between 800 and

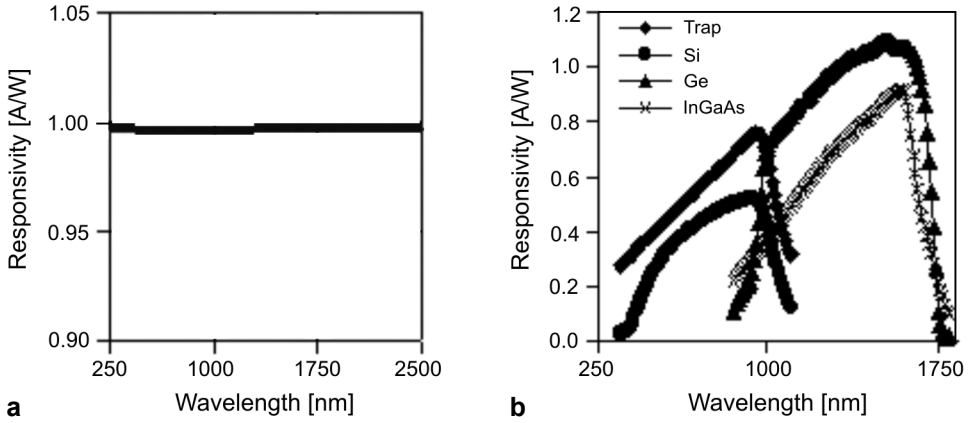


Fig. 8. Spectral responsivity of pyroelectric detector *vs.* wavelength (**a**), responsivities of trap, Si, Ge, InGaAs detectors (**b**).

1800 nm using germanium (Ge) and indium galium arsenide (InGaAs). The relative responsivity of these detectors was measured using substitution method. The substitution method uses a reference detector (RD) to transfer its responsivity to test detector (TD) as given in the following equation

$$R_{\mathrm{TD}}(\lambda) = \frac{V_{\mathrm{TD}}}{V_{\mathrm{RD}}} \frac{G_{\mathrm{RD}}}{G_{\mathrm{TD}}} R_{\mathrm{RD}}(\lambda) \tag{10}$$

where $V_{\mathrm{TD}}$ and $V_{\mathrm{RD}}$ are the output voltages of test and reference detectors, respectively, $G_{\mathrm{RD}}$ and $G_{\mathrm{TD}}$ are gains for transimpedance amplifiers. Here, reference detector is the pyrolectric detector. $R_{\mathrm{TD}}(\lambda)$ is the responsivity of reference detector at the specified wavelength.

## 4. Conclusions

Absolute optical power measurements were achieved at UME by using ESCR at the temperature of liquid helium with $1.2\times10^{-4}$ uncertainties. In the measurements, $Ar^+$, He-Ne and Nd:YAG lasers were used as radiant sources. To generate a geometrically well-defined Gaussian laser beam a laser power stabilizing system that kept the power level stable at about 0.006% was employed.

After optical power measurements, trap and pyroelectric detectors were calibrated against ESCR at $Ar^+$, Nd:YAG and He-Ne laser wavelengths in order to establish absolute responsivity scale. Reflectance and internal quantum efficiency of the trap detector was also obtained at the same laser wavelengths. The calculated values for the reflectance and internal quantum efficiency fitted the measured values with an uncertainty of $10^{-4}$ level. Using the interpolated and extrapolated reflectance and

internal quantum efficiency values the spectral responsivity scale was established in the spectral ranges of 350–850 nm.

The spectral responsivity scale from 250 to 350 nm and from 850 to 2500 nm was realized using ECPR traceable to the ESCR. ECPR was calibrated against ESCR at vertically polarized tuneable $Ar^+$ (488 nm, 514.5 nm) and Nd:YAG (532 nm) and fixed He-Ne (632.8 nm) laser wavelengths with a standard uncertainty of 1.7%. At four laser wavelengths an average calibration factor of 1.005 was found. The relative spectral responsivity of ECPR between 250 and 2500 nm region was determined from spectral reflectance measurement. The reflectance measurements indicated that pyroelectric detector is spectrally flat within 0.1%.

## References

[1] MARTIN J.E., FOX N.P., KEY P.J., Metrologia **21** (1985), 147.
[2] OHNO Y., CROMER C.L., HARDIS C.E., EPPELDAUER G., **23** (1994), 88.
[3] GOODMAN T.M., KEY P.J., Metrologia **25** (1988), 29.
[4] BOIVIN L.P., GAERTNER A.A., GIGNAC D.S., Metrologia **24** (1987), 139.
[5] TOIVANEN P., KARHA P., MANOOCHEHRI F.,IKONEN E., Metrologia **37** (2000), 131.
[6] TIMO VARPULA, HEIKKI SEPPA, JUHA-MATTI SARRI, IEEE Transactions On Instrumentation and Measurement **38** (1989), 558.
[7] ZALEWSKI E.F., DUDA C.R., Appl. Opt. **19** (1983), 2867.
[8] FOX N.P., Metrologia **28** (1991), 197.
[9] GEIST J., Phys. Rev. B **27** (1983), 4841.
[10] KORDE R., GEIST J., Appl. Opt. **26** (1987), 5284.
[11] GARDNER J.L., BROWN W.J., Appl. Opt. **26** (1987), 2431.
[12] DOYL W.M., MCINTOSH B.C., GEIST J., Opt. Eng. **15** (1976), 541.
[13] KÖHLER R., GOEBEL R., PELLOR., Metrologia **33** (1996), 549.
[14] GENTILE T.R., HOUSTON J.M., HARDIS J.E., CROMER C.L., PARR A.C., Appl. Opt. **35** (1996), 1056.
[15] STOCK K.D., HOFER H., Metrologia **30** (1993), 291.
[16] NETTLETON D.H., PRIOR T.R., WARD T.H., Metrologia **30** (1993), 425.
[17] GENTILE T.R., HOUSTON S.M., CROMER C.L., Appl. Opt. **35** (1996), 4392.
[18] DURANT N.M., FOX N.P., Metrologia **30** (1993), 345.
[19] BOIVIN L.P., MCNEELY F.T., Appl. Opt. **25** (1986), 554.
[20] HAAPALINNA A., KARHA P., IKONEN E., Appl. Opt. **31** (1998), 729.
[21] KARHA P., FAGERLUND H., LASSILA A., LUDVIGSEN H., MONOOCHEHRI F., IKONEN E., Opt. Eng. **34** (1995), 2611.
[22] VARPULA T., SEPPA H., SAARI J.-M., IEEE Transactions on Instrumentation and Measurement **38** (1989), 558.
[23] PALMER J.M., Metrologia **30** (1993), 327.
[24] ZALEWSKI E.F., HOYT C.C., Metrologia **28** (1991), 203.
[25] GEIST J., Appl. Opt. **18** (1979), 760.
[26] WERNER L., FISCHER J., JOHANNSEN U., HARTMANN J., Metrologia **37** (2000), 279.
[27] LAASON T.C., BRUCE S., PARR A.C., NIST Special Publication 250-41, 1998, p. 29

*Received April 7, 2004*
*in revised form August 10, 2004*